

Dark curve analysis of thin-film GaAs solar cells, with a focus on photon recycling approaches

Original

Dark curve analysis of thin-film GaAs solar cells, with a focus on photon recycling approaches / Gruginskie, Natasha; Bauhuis, Gerard; Mulder, Peter; Cappelluti, Federica; Vlieg, Elias; Schermer, John. - ELETTRONICO. - (2021), pp. 1065-1068. (Intervento presentato al convegno 2021 IEEE 48th Photovoltaic Specialists Conference (PVSC) tenutosi a Fort Lauderdale, FL, USA nel 2021) [10.1109/PVSC43889.2021.9518568].

Availability:

This version is available at: 11583/2927794 since: 2021-09-28T14:42:51Z

Publisher:

IEEE

Published

DOI:10.1109/PVSC43889.2021.9518568

Terms of use:

This article is made available under terms and conditions as specified in the corresponding bibliographic description in the repository

Publisher copyright

IEEE postprint/Author's Accepted Manuscript

©2021 IEEE. Personal use of this material is permitted. Permission from IEEE must be obtained for all other uses, in any current or future media, including reprinting/republishing this material for advertising or promotional purposes, creating new collecting works, for resale or lists, or reuse of any copyrighted component of this work in other works.

(Article begins on next page)

Dark curve analysis of thin-film GaAs solar cells, with a focus on photon recycling approaches

Natasha Gruginskie¹, Gerard Bauhuis¹, Peter Mulder¹, Federica Cappelluti², Elias Vlieg¹, and John Schermer¹

¹Radboud University Nijmegen - Institute for Molecules and Materials, Applied Materials Science. Heyendaalseweg 135, 6525AJ Nijmegen, The Netherlands. ²Politecnico di Torino, Department of Electronics and Telecommunications, Corso Duca degli Abruzzi 24, I-10129 Torino, Italy

Abstract — Multiple studies have been recently conducted towards increasing photon recycling in thin-film GaAs solar cells. It has been established that the photon recycling probability increases with the rear mirror reflectance and solar cell thickness, which results in the increase of the devices open circuit voltage. However, perimeter and interface recombination have been shown to hinder the internal radiative efficiency of the solar cells, preventing further increase of the devices' performance as a result of improvements to the rear mirror reflectivity. In this study, we present an in-depth analysis of the effects that interface recombination has on the device performance, focused on the solar cells dark characteristics. In order to fully exploit the significant benefit of an increased photon recycling probability to the solar cell performance, these limiting mechanisms need to be properly addressed.

Keywords— GaAs solar cells, photon recycling, thin-film solar cells

I. INTRODUCTION

Thin-film GaAs solar cells achieve the highest efficiency among all single junction solar cell technologies [1, 2]. The thin-film architecture presents many advantages over the substrate-based counterparts, such as the reduced weight and potential of reduced costs with the removal and reuse of the wafer, possibility of utilizing thinner epi-layers with the application of a back reflector that increases the light optical path, increased resilience to particle irradiation for space application [3] due to the reduced thickness, bendability and increased photon recycling due to reflectance of emitted photons.

It has been established [4] that, with the application of a high-quality back reflector, thin-film GaAs solar cells have the potential to reach efficiencies close to the theoretical limit. The reflectance of the back mirror has a direct impact on the solar cell parameters, most drastically affecting the open circuit voltage (V_{oc}), due to a more efficient re-absorption of radiatively emitted photons. In a recent study [5], however, it has been demonstrated that the benefits of photon recycling to the solar cell V_{oc} is dependent on the device operating in a predominantly radiative recombination regime.

In the present study, we show an in-depth theoretical analysis of the solar cell performance, focused on the dark characteristics. A physics-based model is used in order to fit the solar cell parameters and predict the performance of devices

with different structures. Furthermore, a number of solar cells will be fabricated to validate the model simulations.

II. METHODS

A combination of models reported in the literature [6-9] was used in order to simulate different optical and electronic mechanisms of the solar cells. Firstly, the reflectance at the emitter-window (R_f) and at the base-BSF (R_r) interfaces was calculated as a function of photon wavelength and angle of incidence. The required complex refractive index ($n + ik$) data were retrieved from ellipsometry analyses and from the literature [10-13].

The transport and collection of minority carriers are determined by the diffusion length, given by $L_{p(n)} = (D_{p(n)}\tau_{p(n)})^{1/2}$, where the subscript identifies electrons (n) in the base and holes (p) in the emitter. $D_{p(n)}$ is the diffusion coefficient, defined according to the model described by Sotoodeh et al. [9], and $\tau_{p(n)}$ is the minority carrier lifetime, calculated under low injection conditions considering both radiative and defect mediated non-radiative recombination as:

$$\frac{1}{\tau_{p(n)}} = \frac{1-f_{PR}}{\tau_{p(n),rad}} + \frac{1}{\tau_{p(n),SRH}}, \quad (x)$$

where the subscripts *rad* and *SRH* indicate the radiative and Shockley-Read-Hall recombination lifetimes, respectively, and f_{PR} indicates the photon recycling factor, indicating the probability that a photon resulting from radiative recombination is reabsorbed in the active layers of the solar cells [6].

A few solar cells were fabricated in order to provide experimental support to the simulations. The used structure was grown by low-pressure MOCVD on 2-inch diameter GaAs wafers with (1 0 0) 2° off to (1 1 0) orientation. It consists of a thick *n*-doped emitter ($X_E = 2000$ nm, $N_D = 2 \times 10^{17}$ cm⁻³), and a thin *p*-doped base ($X_B = 100$ nm, $N_A = 1 \times 10^{18}$ cm⁻³). Two passivating layers, a 20 nm AlInP window and a 100 nm InGaP back surface field (BSF), were grown enclosing the active layers, in order to repel the minority carriers and reduce surface recombination. The top contact layer consists of 300 nm *n*-GaAs, and for the bottom contact layer, 150 nm Al_xGa_{1-x}As was used, with the fraction of Al x being 0.1 for the outer 20 nm and 0.3 for the remaining 130 nm. The substrate was removed with an aqueous citric acid and hydrogen peroxide solution (5:1 in volume). The rear contact/mirror consists of a continuous Au

layer, and a Cu-foil that acts as a conductive carrier was applied. The structure was processed into $0.5 \times 0.5 \text{ cm}^2$ cells with a front grid coverage (C_f) of 16.6 %. A schematic depiction of the processed solar cells is depicted in figure 1.

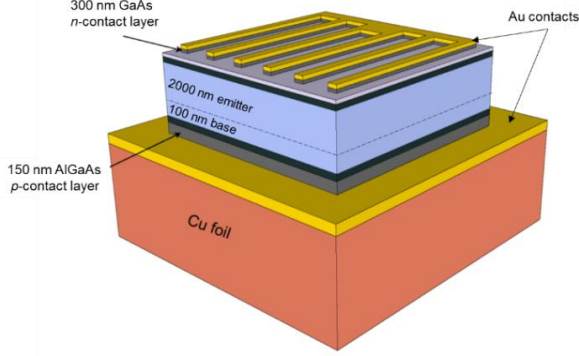


Fig. 1. Schematic depiction of the structure of the fully-processed solar cells used in this study.

III. RESULTS AND DISCUSSION

The overall quality of the solar cells is gauged by the analysis of the devices dark J-V curve. Solar cells in the dark under forward bias are generally analyzed as two diodes in parallel, and after de-embedding the possible influence of the parasitic series and shunt resistances, they are expressed by:

$$J_{\text{dark}} = J_{01} \left(e^{\frac{qV}{kT}} - 1 \right) + J_{02} \left(e^{\frac{qV}{2kT}} - 1 \right), \quad (1)$$

where J_{01} and J_{02} are the saturation current densities of the $1kT$ and $2kT$ components, respectively. In this equation, q is the electron charge, k is the Boltzmann constant, T is the temperature.

At lower voltages, the dark curve is dominated by J_{02} , which represents the non-radiative recombination that takes place predominantly in the space charge region ($J_{0,SCR}$) and at the perimeter ($J_{0,perim}$) of the cell, given as $J_{02} = J_{0,SCR} + J_{0,perim}$. The perimeter recombination fraction is generally not computed in dark curve analysis, but it can account for a large fraction of the dark current of small solar cells, such as the cells applied in CPV systems and the here studied $0.5 \times 0.5 \text{ cm}^2$ devices. In contrast to the other saturation current densities, $J_{0,perim}$ is difficult to predict, since it can vary largely as a function of the quality of the technique that defines the solar cell area (such as the used MESA etchants) [14]. In large area cells, however, J_{02} is likely to be mostly limited by $J_{0,SCR}$.

At higher voltages, on the other hand, the dark curve is dominated by J_{01} , which arises from the recombination of minority carriers in the quasi-neutral regions (QNR) and at the front and rear inter-faces [14-16]. The drift-diffusion theory defines the radiative saturation current density, J_{01} , as:

$$J_{01} = J_{01,E} + J_{01,B}, \quad (3a)$$

with

$$J_{01,E} = \frac{qD_p n_i^2}{L_p N_D} \times \frac{\sinh \frac{d_E}{L_p} + \frac{S_p L_p}{D_p} \cosh \frac{d_E}{L_p}}{\cosh \frac{d_E}{L_p} + \frac{S_p L_p}{D_p} \sinh \frac{d_E}{L_p}}, \quad (3b)$$

and

$$J_{01,B} = \frac{qD_n n_i^2}{L_n N_A} \times \frac{\sinh \frac{d_B}{L_n} + \frac{S_n L_n}{D_n} \cosh \frac{d_B}{L_n}}{\cosh \frac{d_B}{L_n} + \frac{S_n L_n}{D_n} \sinh \frac{d_B}{L_n}}, \quad (3c)$$

where d_E and d_B are the quasi-neutral regions (QNR) of the emitter and base, respectively, and S_p and S_n refer to the interface recombination velocity at the emitter-window and the base-BSF interfaces.

An improved photon recycling increases the minority carriers' lifetime, and therefore will reduce J_{01} . The device's $s f_{PR}$ is directly proportional to the reflectance at the front and rear interfaces and the device thickness. In a previous study [5], it has been demonstrated that, among other parameters, the front grid coverage will directly impact the devices photon recycling, and have no other influence to the cell operation in the dark. Therefore, in figure 2, the calculated J_{01} of a device with a Au mirror and doping parameters similar to the fabricated solar cells is depicted as a function of emitter thickness for different C_f values. This figure clearly shows the decrease in J_{01} as a direct result of an increased f_{PR} due to the reduced front grid. On the other hand, the increase in f_{PR} due to a larger thickness is not sufficient to overcome its negative impacts to the dark curve.

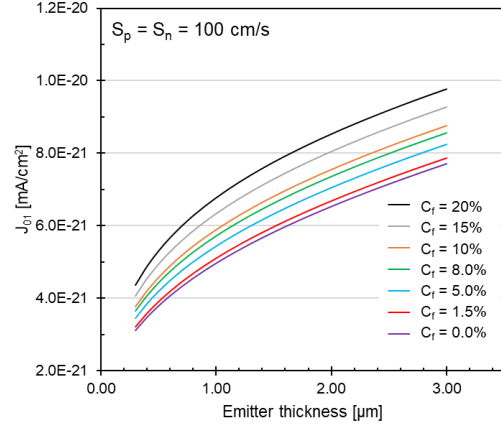


Fig. 2. Modeled radiative saturation current density (J_{01}) of solar cells as a function of emitter thickness, considering different front grid coverages (C_f).

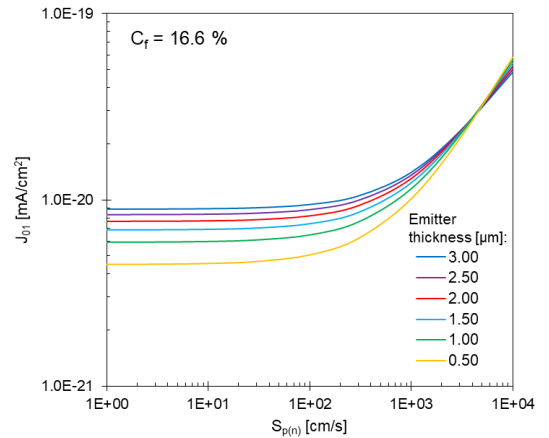


Fig. 3. Modeled radiative saturation current density (J_{01}) of solar cells as a function of interface recombination velocity, considering $S_p = S_n$, for different emitter thicknesses.

The effects of an increased photon recycling can only be observed in solar cells operating on a radiative recombination regime. It has been demonstrated [5] that an important parameter limiting the solar cells output is a non-negligible value for S_p and S_n . In figure 3, the calculated J_{01} for the same structure with different emitter thickness, as a function of $S_{p(n)}$ is depicted. This figure shows that, in order for the interface recombination velocity to have negligible effect in the cell output, its value must be lower than 1×10^2 cm/s.

The illuminated J-V curve of one of the fabricated devices is shown in figure 4, and the extracted illuminated parameter are highlighted. The solar cell presents a high efficiency ($\eta=26.6\%$ when the current is corrected for the active area), but it is not yet operating close to the theoretical limit.

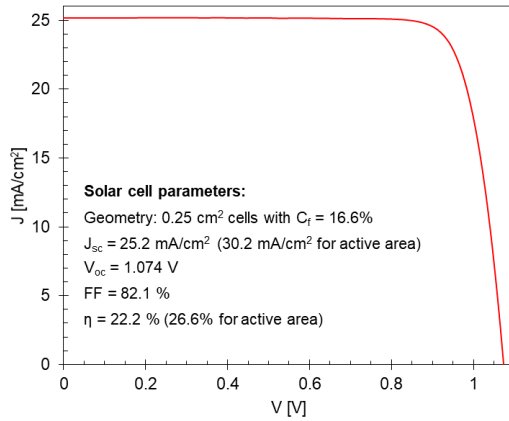


Fig. 4. Illuminated J-V characteristics of a fabricated solar cell, with the extracted parameters highlighted.

For cells where bulk recombination is negligible with respect to the surface recombination, J_{01} can be approximated as the sum of a surface-limited diffusion component ($J_{0,diff}$) and a radiative recombination component ($J_{0,rad}$) [8, 10]. Any improvement to the cells photon recycling probability will only reduce $J_{0,rad}$.

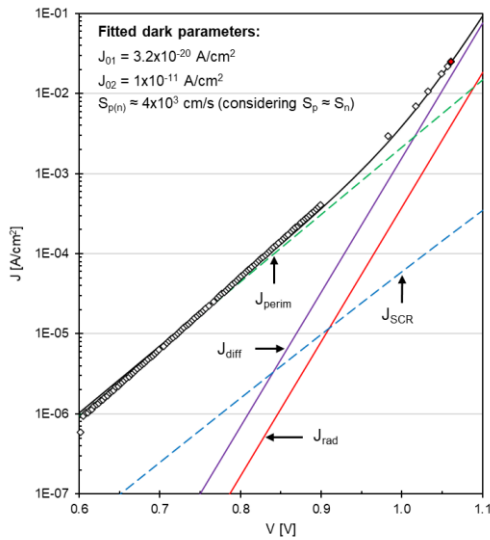


Fig. 5. Experimental (markers) and modeled (black solid line) dark characteristics of the studied thin-film solar cell. The curves are modeled as the

sum of the diffusion (J_{diff} , purple), radiative (J_{rad} , red), perimeter (J_{perim} , green) and space charge region (J_{SCR} , blue) recombination current densities.

The dark J-V characteristics of the fabricated device are shown in figure 5, together with the modelled components of the dark curve. This figure shows that, for this device, $J_{0,diff}$ is larger than $J_{0,rad}$, and is therefore limiting the dark current at higher voltages, which will hinder improvements to the performance due to increased photon recycling.

By fitting the experimentally extracted J_{01} with equations 3a-c, it is evident that the solar cell has $S_{p(n)}$ values in the order of 4×10^3 cm/s, considering $S_p = S_n$. Furthermore, $J_{0,perim}$ is much higher than $J_{0,SCR}$, dominating the dark curve at lower voltages. This effect can potentially be reduced with the fabrication of larger devices or with the application of a surface passivation technique.

CONCLUSIONS

In the presented study, optical and electrical modelling was used in order to gauge the performance of thin-film GaAs solar cells, varying a few design parameters. An in-depth theoretical analysis of the solar cells dark characteristics was used in order to pinpoint limiting mechanisms to photon recycling in the devices. Perimeter and interface recombination seem to be limiting the solar cell operation, preventing the cells to fully benefit from optical improvements. Therefore, a number of experimental devices will be further prepared and analyzed in order to support the calculations, and possibly evaluate which design aspects are increasing interface recombination in the solar cells.

Given the fact that interface recombination is a possible bottleneck to the cells performance, also from a radiation resistance standpoint, a further evaluation and possible improvement of the quality of the top and bottom hetero-interfaces is required.

REFERENCES

- [1] M. A. Green et al. Prog Photovolt Res Appl. 28 (2020) 3–15.
- [2] G. Bauhuis et al. Solar Energy Materials & Solar Cells 93 (2009) 1488–1491.
- [3] N. Gruginskij et al. Prog Photovolt Res Appl. 28(2020)266–278.
- [4] O. D. Miller et al. IEEE Journal of Photovoltaics. 2, no. 3 (2012) 1-27.
- [5] N. Gruginskij et al. Prog Photovolt Res Appl. 2020;1–12.
- [6] M. A. Steiner et al. Journal of Applied Physics. 113 (2013) 123109(1-11).
- [7] M.P. Lumb et al. Journal of Applied Physics 116 (2014) 194504(1-10).
- [8] Y. Sun et al. IEEE Journal of Photovoltaics. (2019) 9(2):437-445.
- [9] M. Sotoodeh et al. J Appl Phys. 2000;87(6):2890-2900
- [10] S. Adachi. J Appl Physiol. (1985) 58(3):1-29.
- [11] E.D. Palik. Handbook of Optical Constants of Solids. Vol 3. Cambridge,Massachusetts: Academic Press (1998).
- [12] Y. Jiang et al. Scientific Reports (2016) 6:30605.
- [13] Sopra n-k database. <http://www.sspectra.com/sopra.html>.
- [14] Ochoa M, et al. Sol Energy Mater Sol Cells. 2014;120:48-58.
- [15] H.J. Hovel; Semiconductors and Semimetals, Vol. II: Solar cells.New York: Academic Press; 1975.37.
- [16] J. Nelson. The Physics of Solar Cells. London: Imperial College Press;2003.